Universidad de Zaragoza

End-of-Degree Thesis

Study of an inhomogeneous spin-orbit coupling in topological semiconducting wires

Author:
Mateo Uldemolins Nivela

Supervisor:
Prof. Pascal Simon

Laboratoire de Physique des Solides

Université Paris-Sud

22 June 2019

Study of an inhomogeneous spin-orbit coupling in topological semiconducting wires

Abstract

The present End-of-Degree Thesis is framed within the context of Majorana fermions in Condensed Matter, and it focusses on the Rashba nanowire, a realistic system which allows the emergence of *Majorana zero modes*. After having introduced the present state of affairs in the field, the original proposal is reviewed, and subsequently, a nanowire with inhomogeneous spin-orbit coupling is analysed. Utilizing numerical techniques, it is shown that under precise conditions a defect in the spin-orbit coupling can originate zero-energy *fermionic bound states* akin to the original Majorana zero modes. Finally, a finite-size effect induced by the presence of the defect is investigated.

Acknowledgements

I would like to express my profound gratitude to my supervisor Pascal Simon and his colleague Andrej Mesaros for their tireless mentorship during the past months, and also, for their warm welcome at the Group. Many thanks as well to Arfor, Toni, Jean-Baptiste and the other fellow interns for the insightful discussions, and especially, for brightening up the days at the office.

Moreover, as this work is the last piece of a four-year-long endeavour, I would also like to devote some lines to mention my friends and colleagues Fernando, Juan and Marcos, with whom I shared the journey; and above all, to thank my parents for their encouragement and endless support.

Preface for the version uploaded to the Universidad de Zaragoza archive

This End-Of-Degree Thesis ought to be understood as the combination of two self-contained pieces. The elaboration of the main work (*Study of an inhomogeneous spin-orbit coupling in topological semiconducting wires*) was preceded by an introductory bibliographical survey on the topic. The report which details this initial work (*Introduction to Topological Bound States*) has been incorporated as an appendix of the main body owing to bureaucratic matters; nevertheless, both texts can be considered independently, having their own introduction and bibliography, and existing some partial overlapping of content.

The two projects were conducted at the Laboratoire de Physique des Solides in Orsay during 2019 under the supervision of Prof. Pascal Simon.

Contents

Chapter 1

Introduction

Almost a century ago, the Italian physicist Ettore Majorana introduced the concept of *Majorana fermions*, particles which would constitute their own antiparticles. The search of these hypothetical entities in the field of high energy physics has been hitherto fruitless, however, in the past few decades, condensed matter systems have proved a promising platform for their study [1–3].

Nonetheless, in the field of solid state physics, Majorana fermions are not elementary particles as originally envisaged by E.M., but rather, quasi-particle excitations of a many-body ground state which ultimately amount to a certain combination of electrons and holes. This inevitable feature hinders the quest: in a simple metal, charge renders electrons ($c_\sigma^\dagger$) different from their hermitian conjugate, holes (c_σ), and so does spin in the Bogoliubov operators ($d = uc_\uparrow^\dagger + vc_\downarrow$) underpinning typical, s-wave superconductors. The previous observation suggests that effective *spinless* superconductors could be adequate candidates to host Majorana fermions [3]. Indeed, as it was shown by A. Kitaev [4], under precise conditions, p-wave superconductors in 1D allow the emergence of zero-energy modes which fulfil the Majorana formal requirement $\gamma = \gamma^\dagger$. Their two-dimensional analogue $(p_x \pm ip_y)$-wave superconductors are also useful to that purpose, but regrettably, such materials are scarce in nature, and to this date, only Sr_2RuO_4 has been predicted to exhibit intrinsic triplet pairing [3].

This demoralizing gloom was finally driven away after the groundbreaking work by Fu and Kane, where they showed that it was possible to obtain a two dimensional state hosting Majorana bound states at vortices by proximitizing an ordinary s-wave superconductor to a strong topological insulator [5]. This concept was thereupon refined and other proposals followed: first, semiconductor-superconductor heterostructures [6], and then, the further simplified one-dimensional nanowires [7, 8].

The underlying idea of the preceding examples is to engineer p-wave superconductivity by effectively disposing of the electron's spin degree of freedom. In the scheme proposed by Oreg *et al.* [8] this is achieved by combining spin-orbit coupling with an external magnetic field. The first ingredient splits the spectrum in two bands whose spin depends on the momentum, while the second breaks time-reversal symmetry, lifting Kramer's degeneracy. This solves the fermion doubling problem and eventually allows s-wave superconductivity to induce the desired p-wave-like pairing mechanism.

Among the vast quantity of recent advancements which constitute the state-of-the-art in the field of Majorana fermions, this End-Of-Degree Thesis will be focused on their occurrence in one-dimensional systems. Accordingly, our starting point will be the Kitaev chain, a toy model which exemplifies the emergence of Majorana zero modes on the edges of a topological p-wave superconductor. Later, a substantial part of this work will be devoted to review the scheme described in the preceding paragraph, and at last, we will explore the consequences of introducing a certain degree of inhomogeneity in the spin-orbit coupling field.

In order to conclude these introductory lines, it is perhaps worth mentioning why the Majorana fermions have attracted this great deal of attention among the research community in Condensed Matter. Aside from their fundamental interest, the collective excitations identified with the Majorana fermions have the property of exhibiting non-Abelian statistics. Unlike many-body systems whose behaviour is dictated by the usual fermionic or bosonic statistics, the wavefunction of these exotic anyons can experience a fundamental alteration under the exchange of the constituents, a feature which renders them promising candidates to embody the so-called *Topological Quantum Computation* [3]. Furthermore, Majorana zero modes have been proposed as a decoherence-protected alternative to store quantum information [4].

1.1 Presenting the Majorana fermions: The Kitaev chain

Throughout this Section we will examine the system proposed by A. Kitaev, which is probably the simplest model to date supporting the existence of Majorana zero modes (MZMs). However, before introducing the Hamiltonian of the model, discussing some generalities about the MZMs is in order.

Formally speaking, the *Majorana operators* ($\gamma_{Aj},\ \gamma_{Bj}$) can be understood as a "decomposition" of the ordinary fermionic operators in their real and complex parts,

$$c_j^\dagger = \frac{1}{2}\left(\gamma_{Aj} + i\gamma_{Bj}\right), \qquad c_j = \frac{1}{2}\left(\gamma_{Aj} - i\gamma_{Bj}\right). \tag{1.1}$$

As opposed to the typical fermionic anti-commutativity ($\{c_i, c_j\} = \{c_i^\dagger, c_j^\dagger\} = 0,\ \{c_i, c_j^\dagger\} = \delta_{ij}$), the Majorana operators fulfil the relations

$$\{\gamma_{\alpha i}, \gamma_{\beta j}\} = 2\delta_{\alpha\beta}\delta_{ij}, \qquad \gamma_{Aj}^2 = \gamma_{Bj}^2 = 1. \tag{1.2}$$

Furthermore, from their definition in Eq. (1.1), one can observe that these new operators are hermitian, i.e., $\gamma_{Aj}^\dagger = \gamma_{Aj}$ and $\gamma_{Bj}^\dagger = \gamma_{Bj}$. This remarkable fact has two important consequences. Firstly, it does not allow to think of a Majorana mode as being filled or empty, a property we shall reserve for fermionic modes. Secondly, since electrons and holes are their respective hermitian conjugates, it will be natural to search for Majorana zero modes at the Bogoliubov quasi-particle excitations of a superconductor, which have both electron and hole components.

A careful inspection of the previous definition, leads us to realize that physical systems will always have an even number of Majorana operators. Naively, we might think that each pair of Majoranas will be always localized in their corresponding fermionic site, but as we will see, certain systems allow isolated Majorana modes to arise.

To that purpose, Kitaev proposed a toy model which is essentially a tight-binding description of a one-dimensional spinless p-wave superconductor. The Hamiltonian writes [4],

$$H = -\mu \sum_{j=1}^{N} \left(c_j^\dagger c_j - \frac{1}{2} \right) + \sum_{j=1}^{N-1} \left[-t \left(c_j^\dagger c_{j+1} + c_{j+1}^\dagger c_j \right) + \Delta c_j c_{j+1} + \Delta^* c_{j+1}^\dagger c_j^\dagger \right], \quad (1.3)$$

where t is the hopping amplitude, μ is the chemical potential, Δ the induced superconducting gap and N is the number of sites in the chain. The mechanism of superconductivity is not crucial for this initial analysis, we will just assume that our wire is in contact with some bulk superconductor which injects and extracts Cooper pairs. We shall however remark, that the Pauli exclusion principle together with the spinless nature of our chain forces the superconducting pairing to be between next-neighbour sites. Finally, we can assume the pairing parameter Δ to be real, or equivalently, absorb its complex phase in the definition of the Majorana operators.

Following Kitaev's steps, let us insert the Majorana operators (Eq. (1.1)) in the previous expression and rewrite the Hamiltonian as follows,

$$H = -\frac{i\mu}{2} \sum_{j=1}^{N} \gamma_{Aj} \gamma_{Bj} + \frac{i}{2} \sum_{j=1}^{N-1} \left[(t + |\Delta|) \gamma_{Bj} \gamma_{Aj+1} + (-t + |\Delta|) \gamma_{Aj} \gamma_{Bj+1} \right]. \quad (1.4)$$

In order to better grasp the topological properties of the Kitaev model, we shall start by analysing the previous equation in two limiting cases [4, 9]:

If $|\mathbf{\Delta}| = \mathbf{t} = \mathbf{0}$ $\mu < \mathbf{0}$, the system is in the **trivial phase**, and the Hamiltonian reads,

$$H_{triv} = -\frac{i\mu}{2} \sum_{j=1}^{N} \gamma_{Aj} \gamma_{Bj}, \quad (1.5)$$

where only Majorana operators of the *same site* j are paired together.

However, if we set $|\mathbf{\Delta}| = \mathbf{t} > \mathbf{0}$ $\mu = \mathbf{0}$, the system enters a different regime, the so-called **topological phase**. In this case,

$$H_{topo} = it \sum_{j=1}^{N-1} \gamma_{Bj} \gamma_{Aj+1}. \quad (1.6)$$

Now the Majorana operators from *different sites* are paired together, contrary to the previous case, where same site Majorana operators were coupled to form a stan-

dard fermion. Interestingly, the Majorana operators γ_{A1} and γ_{BN} remain unpaired, and therefore $[H_{topo}, \gamma_{A1}] = [H_{topo}, \gamma_{BN}] = 0$.

As it was mentioned a few paragraphs above, the definition of the Majorana operators (Eq. (1.1)) shows that each of them only represents half of a fermionic degree of freedom. Thus, it seems reasonable to define a complex operator combining the coupled Majoranas from the Hamiltonian (1.6),

$$d_j^\dagger = \frac{1}{2}\left(\gamma_{Bj} - i\gamma_{Aj+1}\right), \qquad d_j = \frac{1}{2}\left(\gamma_{Bj} + i\gamma_{Aj+1}\right). \tag{1.7}$$

These operators describe fermionic excitations, and more specifically, they are the Bogoliubov quasi-particles which diagonalize the topological Hamiltonian

$$H_{topo} = 2t \sum_{j=1}^{N-1} \left(d_j^\dagger d_j - \frac{1}{2} \right). \tag{1.8}$$

Remarkably, the previous Hamiltonian only involves $N-1$ fermionic excitations, whereas the original chain had N sites. This situation stems from the fact that the Majorana operators γ_{A1} and γ_{BN} did not enter the Hamiltonian in the topological phase. Certainly, we are allowed to define another fermionic operator relating these two Majoranas in like manner,

$$d_0^\dagger = \frac{1}{2}\left(\gamma_{A1} - i\gamma_{BN}\right), \qquad d_0 = \frac{1}{2}\left(\gamma_{A1} + i\gamma_{BN}\right), \tag{1.9}$$

which is highly delocalized and has zero energy. The latter property implies that the ground state is two-fold degenerate. It will be constructed "subtracting" from the vacuum the Bogoliubov quasi-particles of energy t, and there will always exist the freedom to "add" the excitation defined in Eq. (1.9), since it has zero energy. These two states read,

$$|\psi_0\rangle = d_0 \prod_{j=1}^{N-1} d_j \, |\text{vac}\rangle, \qquad |\psi_1\rangle = d_0^\dagger \, |\psi_0\rangle, \tag{1.10}$$

and have the particularity of differing in the fermionic parity. This property lays bare the difference of our system to conventional superconductors, where the ground state is unique and has even parity, allowing the electrons to pair up into Cooper pairs.

Additionally, the construction of the zero-energy excitation (Eq. (1.7)) sheds some light on the need for spinless fermions in Kitaev's model. Had we considered a spinful chain, the degeneracy of each eigenstate would be doubled, and the chain edges would host *two* Majorana zero modes each, or in other words, a localized fermionic excitation, lacking of any interest [3].

So far, only the special case $|\Delta| = t = 0$ was considered, but in his original paper, A. Kitaev studied analytically the topological phase transition in the parameter space. However, in this introductory survey, we opted for a brief numerical analysis which might provide a clearer insight into the physics of the model. To that purpose, we

shall rewrite the original Hamiltonian in the Bogoliubov-de Gennes formalism [10], i.e. $H = \frac{1}{2} C^\dagger H_{BdG} C$ up to an unimportant constant, being $C = \left(c_1, \dots c_N, c_1^\dagger \dots c_N^\dagger\right)^T$ our choice for the Nambu spinors. The BdG Hamiltonian writes,

$$H_{BdG} = -\mu \sum_{j=1}^{N} \tau_z \left|j\right\rangle \left\langle j\right| - \sum_{j=1}^{N-1} \left[(t\tau_z + i\Delta\tau_y) \left|j\right\rangle \left\langle j+1\right| + \text{h.c.}\right], \tag{1.11}$$

where τ_i are the Pauli matrices acting on particle-hole space, $|j\rangle$ is a N-dimensional column vector representing the j-th site of the chain, and Δ was assumed to be real.

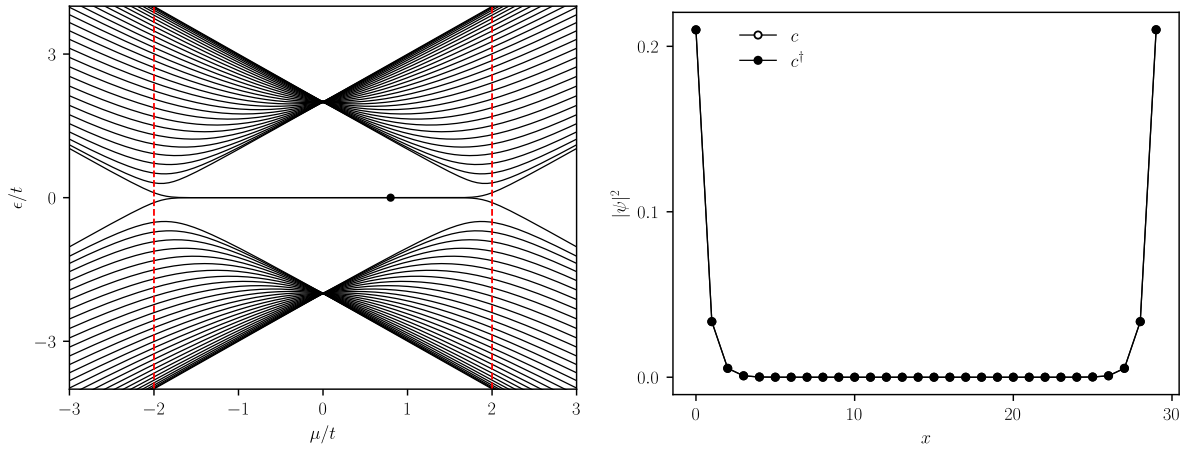

(a) Bogoliubov-de Gennes excitation spectrum as a function of the chemical potential μ. The dashed vertical lines represent the topological phase transition points in the thermodynamic limit.

(b) Eigenmode corresponding to the black dot in the left plot. The markers corresponding to creation and annihilation operators are perfectly superimposed for every x.

Figure 1.1: Numerical analysis for the Kitaev chain ($N = 30$ sites). The superconducting gap Δ is set to 1 in units of t, the hopping parameter.

The spectrum in Figure 1.1a shows the two topological phases that were discussed previously. For $2t > |\mu|$ we observe the trivial phase, where there are not any zero-modes. As we decrease $|\mu|/t$ a zero-mode arises. The phase boundary is given by the equation $2t = |\mu|$ in the limit $N \to \infty$. It is also pertinent to remark that the spectrum is symmetric due to the particle-hole symmetry induced by the BdG formalism. Moreover, the zero-energy level appears to be doubly degenerate, but this is again a consequence of the formalism and it must not be confused with the double-degeneracy of the ground state discussed in Eq. (1.10). In fact, the ground state manifold $(|\psi_0\rangle\,,\ |\psi_1\rangle)$ is a truly many-body state and the previous spectrum only provides the single-particle fermionic excitations over the ground state. Therefore, the zero-energy "state" in the spectrum represents in reality the zero-energy excitation defined in Eq. (1.9), which can be seen in the plot at the right panel (Fig. 1.1b).

The plotted eigenmode is slightly delocalized and decays into the bulk of the chain due to finite-size effects (as a matter of fact, the chain can still be consider topological but one has to go to the thermodynamic limit to find the "proper" edge physics). For that reason, the degeneracy in the ground state is lifted by an energy which scales with

$e^{-L/\xi}$, where L is the length of the chain and ξ is the coherence length (which diverges at the topological phase transition) [3].

We shall finish this introduction inspecting the bulk spectrum of the system, for which we will assume periodic boundary conditions [9, 10]. The Kitaev chain exhibits translational symmetry, therefore we can re-express the Bogoliubov Hamiltonian (1.11) in momentum space, i.e., $H_{BdG} = \sum_k H(k) c_k^\dagger c_k$, where $c_k = \frac{1}{\sqrt{N}} \sum_j e^{-ikj} c_j$, taking the lattice parameter to be the unity for simplicity. From Eq. (1.10) one finds that $H(k)$ is the following 2 by 2 matrix,

$$H(k) = -(\mu + 2t\cos k)\tau_z + 2\Delta \sin k \tau_y, \tag{1.12}$$

whose spectrum is given by

$$E = \pm\sqrt{4\Delta^2 \sin^2 k + (\mu + 2t\cos k)^2}, \tag{1.13}$$

where $k \in (-\pi, \pi)$ in the continuum limit. We are mainly interested in the set of points in the parameter space which correspond to gap closings. Assuming that the superconducting gap is non-zero, the first addend vanishes for $k = 0$ and $k = \pi$, which implies that $\mu = \pm 2t$ for the cosine term to disappear. Those are indeed the points at which we claimed the topological phase transition would happen in the thermodynamic limit (recall spectrum in Figure 1.1a), and the coincidence is not merely accidental. Actually, it is a manifestation of the so-called *bulk-edge correspondence*, which will allow us to relate the topological phase transitions in the open system to the gap-closings in the bulk.

The topological states of matter constitute a field of study on its own which will not be manifestly addressed within this work. Yet, it is worth mentioning that whereas in the classical Ginzburg-Landau theory of spontaneous symmetry breaking, phase transitions are characterised by a *local* order parameter, the topological analogues require a *global* quantity to be described [11]. Indeed, the quasi-particle excitations constituting the Majoranas are massless, chargeless, spinless, and devoid of any local observable. In our system, the relevant quantity is the topological invariant $M = (-1)^\nu$, being ν the number of pairs of Fermi points, which is odd in the topological phase and even otherwise [9].

In order to conclude this introduction, let us emphasize that in spite of its richness, the Kitaev chain is a mere toy model specifically designed to exemplify the existence of unpaired Majorana zero modes. Nonetheless, as it was discussed at the beginning of the Chapter, this does not entail the impossibility to realize such system in the laboratory; on the contrary, it suggests the experimentalist the requisites to observe isolated Majorana zero modes. It will be the goal of the subsequent chapters to explore a feasible proposal to engineer such modes.

Chapter 2

The Rashba nanowire: homogeneous spin-orbit coupling

In the present chapter we will examine one of the many proposals to devise a realistic system capable of hosting Majorana zero modes, and which only requires three simple ingredients: a 1D quantum wire with Rashba spin-orbit coupling (eg. InAs or InSb), a uniform magnetic field and a conventional s-wave superconductor.

As depicted in Figure 2.1, the semiconducting wire is supposed to be placed on a bulk s-wave superconductor, and superconductivity is induced in the wire by proximity effect. Nevertheless, in this work we will address neither the microscopic origin of this mechanism, nor that of the Rashba spin-orbit coupling. Instead, we will consider the Hamiltonian of the system as the starting point, and we will study the role played by each constituent in recreating p-wave superconductivity.

The scheme was originally envisioned by Lutchyn *et al.* [7] and Oreg *et al.* [8]. It has been amply reviewed ever since [3, 9, 11].

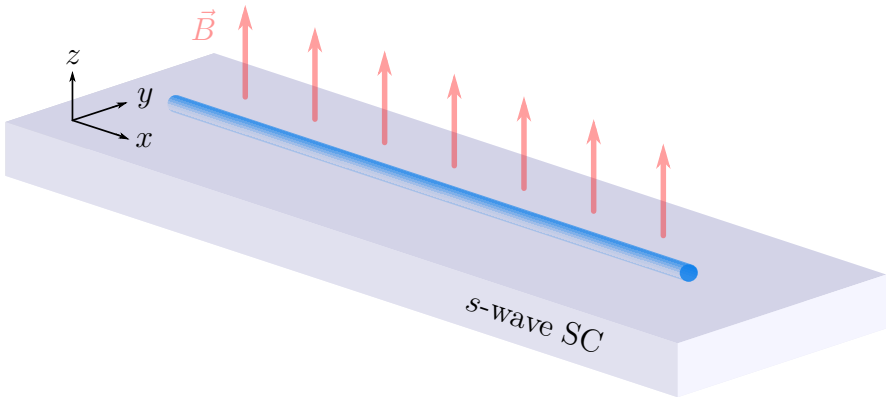

Figure 2.1: Schematic representation of Oreg's proposal. The semiconducting nanowire (in blue) is placed in contact with an s-wave superconductor (in grey). In this work we chose the Rashba spin-orbit coupling to be confined in the $x-y$ plane, whereas the magnetic field is set along the z direction. When the system reaches the topological phase, the MZMs arise on the edges of the nanowire.

Let us start writing explicitly the full Hamiltonian of the system, for which we shall choose $\mathbf{\Psi}^\dagger = (\psi_\uparrow^\dagger, \psi_\downarrow^\dagger, \psi_\downarrow, -\psi_\uparrow)$ as the Nambu spinors.

$$H = \frac{1}{2}\int dx \mathbf{\Psi}^\dagger(x)\left(\mathcal{H}_{kin} + \mathcal{H}_{soc} + \mathcal{H}_{Zeeman} + \mathcal{H}_{sc}\right)\mathbf{\Psi}(x), \tag{2.1}$$

where $\Psi_{\uparrow,(\downarrow)}^\dagger$ creates spin-up (down) electrons at position x, and without loss of generality, we assume our wire to lie along the x axis. The kinetic term writes

$$\mathcal{H}_{kin} = \left(-\frac{\hbar^2\partial_x^2}{2m} - \mu\right)\tau_z\sigma_0, \tag{2.2}$$

where m is the electron's effective mass and μ stands for the chemical potential. The spin-orbit coupling is described by

$$\mathcal{H}_{soc} = -\frac{\alpha}{\hbar}\tau_0\left(\cos\theta\sigma_x + \sin\theta\sigma_y\right)\left(-i\hbar\partial_x\right), \tag{2.3}$$

where α represents the strength of the Rashba field and $\mathbf{u} = (\cos\theta, \sin\theta)$ determines its direction. Note also the presence of the momentum operator, $-i\hbar\partial_x$. In short, this interaction tends to align the x (or y) projection of the electron's spin along the direction of its momentum. We have chosen to analyse the quasi-general case for later purposes (*cf.* Chapter 3), but nothing prevents us from restricting the field to one axis. In this case, the magnetic field is applied perpendicular to the wire, along the z axis, and it enters the Hamiltonian as

$$\mathcal{H}_{Zeeman} = B\tau_0\sigma_z, \tag{2.4}$$

where B is the Zeeman energy, and finally, for the superconducting term we have

$$\mathcal{H}_{sc} = \Delta\tau_x\sigma_0, \tag{2.5}$$

where Δ is the induced superconducting gap, assumed to be real. For all the previous expressions $\sigma_{i=0,x,y,z}$ are the Pauli matrices acting on spin space, and $\tau_{i=0,x,y,z}$ their particle-hole counterparts.

In the first place, let us analyse the Hamiltonian corresponding to the nanowire arrangement in the absence of the superconductor, in order to elucidate why our system can be finely tuned to behave as a spinless wire. This simplification allows us to dispense with the BdG formalism and reduce our problem to spin space. Furthermore, assuming an infinite wire, translational invariance enables us to solve the eigenvalue problem in momentum space. The Hamiltonian density to be considered is

$$\mathcal{H}_0 = \xi(k)\sigma_0 - \alpha k\left(\cos\theta\sigma_x + \sin\theta\sigma_y\right) + B\sigma_z, \tag{2.6}$$

where we denoted $\xi(k) = \frac{\hbar^2k^2}{2m} - \mu$ to lighten notation, and the spectrum reads

$$E_\pm(k) = \xi(k) \pm \sqrt{B^2 + k^2\alpha^2}. \tag{2.7}$$

In the absence of Rashba spin-orbit coupling and magnetic field, our spectrum would be the well-known spin-degenerated, parabolic curve corresponding to free electrons, therefore, we would have an even number of pairs of Fermi points (namely two of them)

as depicted at the top-left panel in Fig. 2.2.

Switching on the Rashba field while still maintaining a null Zeeman field lifts the spin degeneracy and the spectrum has two parabolas shifted along the momentum axis by $\pm k_{SO} = \frac{m\alpha}{\hbar^2}$. Each of them corresponds to the spin-up and spin-down projections along the quantization axis determined by the Rashba field $\mathbf{u} = (\cos\theta, \sin\theta)$. However, this is not sufficient to effectively freeze out one of the two spin species, since for any value of the Fermi level above the bottom of the parabolas, both bands would be filled (Fig. 2.2, top-right).

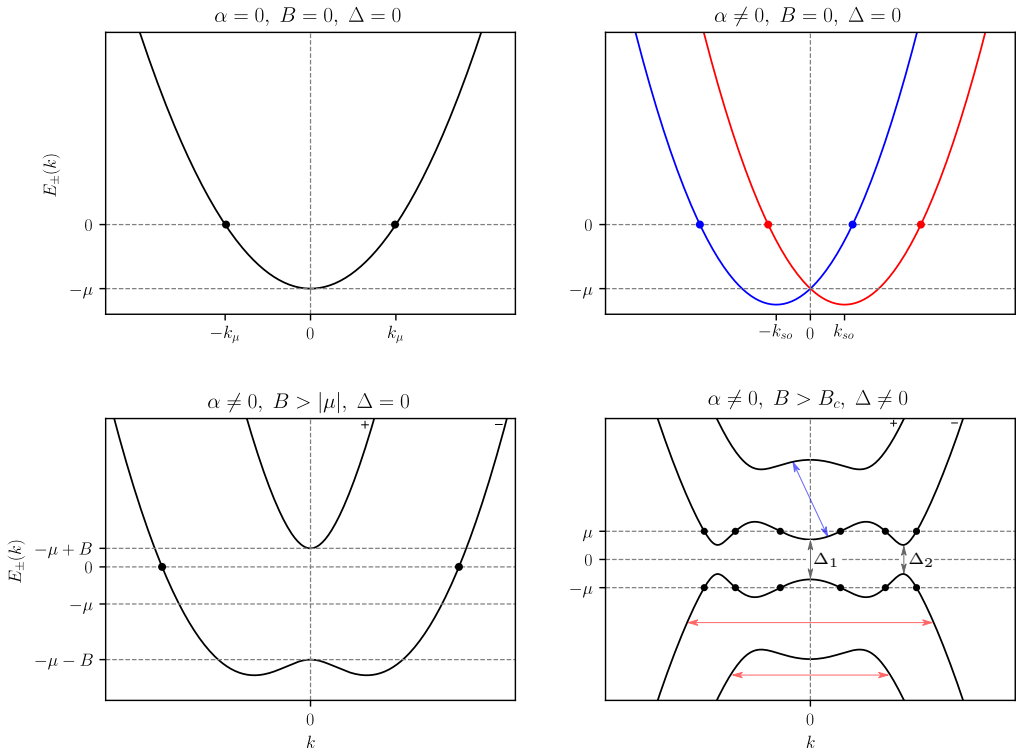

Figure 2.2: Energy bands in momentum space for a Rashba nanowire. Axes in arbitrary units. Adapted from Ref. [11]. **Top-left:** spin-orbit coupling, Zeeman field and superconductivity are set to zero. **Top-right:** A non-vanishing SOC field is considered. The red parabola contains the electronic states with a positive spin projection along the Rashba quantization axis, $\boldsymbol{\alpha}$, and the blue parabola corresponds to their negative counterpart. **Bottom-left**: a magnetic field is applied. **Bottom-right:** superconductivity is taken into account, and the BdG formalism renders the spectrum "doubled". The arrows in red and blue indicate respectively an example of *intraband* pairing (akin to p-wave pairing) and *interband* pairing (Eq. (2.9)).

The situation ameliorates if we apply an external magnetic field which opens a gap of $2B$ at $k = 0$, removing the band crossing, and hence lifting the spin degeneracy at zero momentum (Fig. 2.2, bottom-left). More importantly, since the Zeeman and the Rashba fields are orthogonal to each other, they tend to align the spin along different quantization axis which results in spin-momentum locked bands: the larger the mo-

mentum, the more tilted along the Rashba axis the spin is. Now, it suffices to tune the chemical potential to be inside the Zeeman gap, i.e. $|\mu| < B$, for the system to host an odd number of pairs of Fermi points, which indicates that we are on the right path towards p-wave superconductivity.

In order to illustrate the effective p-wave pairing it is helpful to write the superconducting term defined in Eq. (2.5) in the so-called *helical basis*, which rendered diagonal the wire Hamiltonian (Eqs. (2.6) and (2.7)):

$$\phi_\pm = b_\pm \begin{pmatrix} \gamma_\pm(k) \\ 1 \end{pmatrix}, \quad \text{with} \;\; \gamma_\pm(k) = \frac{\alpha k(-\cos\theta + i\sin\theta)}{-B \pm \sqrt{B^2 + k^2\alpha^2}}, \tag{2.8}$$

where $b_\pm$ are the normalization constants. The superconducting term reads

$$H_{sc} = \Delta_{--}\Psi^\dagger_-(k)\Psi^\dagger_-(-k) + \Delta_{++}\Psi^\dagger_+(k)\Psi^\dagger_+(-k) + \Delta_{+-}\Psi^\dagger_+(k)\Psi^\dagger_-(-k) + h.c., \tag{2.9}$$

where $\Delta_{--} = \frac{-\Delta\gamma_+(k)}{(\gamma_+(k)-\gamma_-(k))^2}$, $\Delta_{++} = \frac{-\Delta\gamma_-(k)}{(\gamma_+(k)-\gamma_-(k))^2}$, and $\Delta_{+-} = \frac{\Delta(\gamma_+(k)+\gamma_-(k))^2}{(\gamma_+(k)-\gamma_-(k))^2}$.

The expression of the Hamiltonian in the new basis makes explicit the effective p-wave superconductivity: indeed, the system still presents an *inter-band pairing* (Δ_{+-}) in a similar fashion to the original s-wave mechanism, but remarkably, electrons from the same spin-momentum locked bands are also paired together via the *intra-band pairing* (Δ_{--}, Δ_{++}). Note that the pairing continues to be between electrons of opposite momentum.

From the previous analysis, it is possible to understand that projecting the initial Hamiltonian (2.1) onto the lower band "$-$", we essentially recover the Kitaev Hamiltonian, a valid operation inasmuch the induced Zeeman gap is sufficiently strong [11].

To gain further insight, we shall go back to the full Hamiltonian (2.1) and calculate the BdG spectrum:

$$E^2_\pm(k) = \xi^2(k) + \alpha^2k^2 + B^2 + \Delta^2 \pm 2\sqrt{B^2\Delta^2 + \xi^2(k)\,(B^2 + \alpha^2k^2)}. \tag{2.10}$$

As a consequence of the superconducting term, the spectrum is now gapped at two points, near $k = 0$ and around the Fermi momentum (bottom-right panel in Fig. 2.2) only the former being relevant for the topological phase transition [8]. The preceding expression evaluated at zero momentum yields

$$E_\pm(k = 0) = \left|B \pm \sqrt{\Delta^2 + \mu^2}\right|, \tag{2.11}$$

and indeed the lower band "$-$" closes at $B = B_c \equiv \sqrt{\Delta^2 + \mu^2}$. In a similar fashion to the bulk-edge correspondence in the Kitaev chain discussed at the end of Section 1.1, this point signals the topological phase transition. This conclusion is in perfect agreement with the previous analysis of the Rashba nanowire in the absence of a bulk superconductor, from which we concluded that for $B > |\mu|$ the system is susceptible of

hosting a topological phase.

We shall finish this Chapter by overcoming the problem numerically. To that purpose, let us formulate a tight-binding model of the system, which can be obtained discretizing the Hamiltonian in Eq. (2.1). Denoting $C_j^\dagger = (c_{j\uparrow}^\dagger, c_{j\downarrow}^\dagger)$ the creation operators for a spin-up(down) electron at position j, the Hamiltonian reads,

$$\begin{aligned} H = &\sum_{j=0}^{N-1} \left[(t-\mu)\, C_j^\dagger \sigma_0 C_j + B C_j^\dagger \sigma_z C_j \right] + \\ &+ \sum_{j=0}^{N-2} \left(-\frac{t}{2} C_{j+1}^\dagger \sigma_0 C_j - \frac{i t_{SO_x}}{2} C_{j+1}^\dagger \sigma_x C_j - \frac{i t_{SO_y}}{2} C_{j+1}^\dagger \sigma_y C_j + h.c. \right) + \\ &+ \sum_{j=0}^{N-1} \Delta \left(c_{j\uparrow}^\dagger c_{j\downarrow}^\dagger + c_{j\downarrow} c_{j\uparrow} \right), \end{aligned} \tag{2.12}$$

where t is the kinetic hopping amplitude, and t_{SO_x}, t_{SO_y} are the spin-orbit coupling hopping parameters. Within the Bogoliubov-de Gennes formalism the matrix to diagonalize is essentially a $4N$ by $4N$ block tridiagonal matrix. Choosing $\mathbf{C}^\dagger = \left(c_{0\uparrow}^\dagger, c_{0\downarrow}^\dagger, c_{0\downarrow}, -c_{0\uparrow}, \cdots, c_{N-1\uparrow}^\dagger, c_{N-1\downarrow}^\dagger, c_{N-1\downarrow}, -c_{N-1\uparrow} \right)$ for the Nambu basis, the block in the diagonal reads

$$D = \begin{pmatrix} t-\mu+B & 0 & \Delta & 0 \\ 0 & t-\mu-B & 0 & \Delta \\ \Delta & 0 & -t+\mu+B & 0 \\ 0 & \Delta & 0 & -t+\mu-B \end{pmatrix}, \tag{2.13}$$

whereas the block in the upper diagonal has the form,

$$U = \frac{1}{2} \begin{pmatrix} -t & t_{SO_y} + i t_{SO_x} & 0 & 0 \\ -t_{SO_y} + i t_{SO_x} & -t & 0 & 0 \\ 0 & 0 & t & -t_{SO_y} - i t_{SO_x} \\ 0 & 0 & t_{SO_y} - i t_{SO_x} & t \end{pmatrix}. \tag{2.14}$$

Necessarily the block in the lower diagonal is $U^\dagger$, so that the Hamiltonian is hermitian.

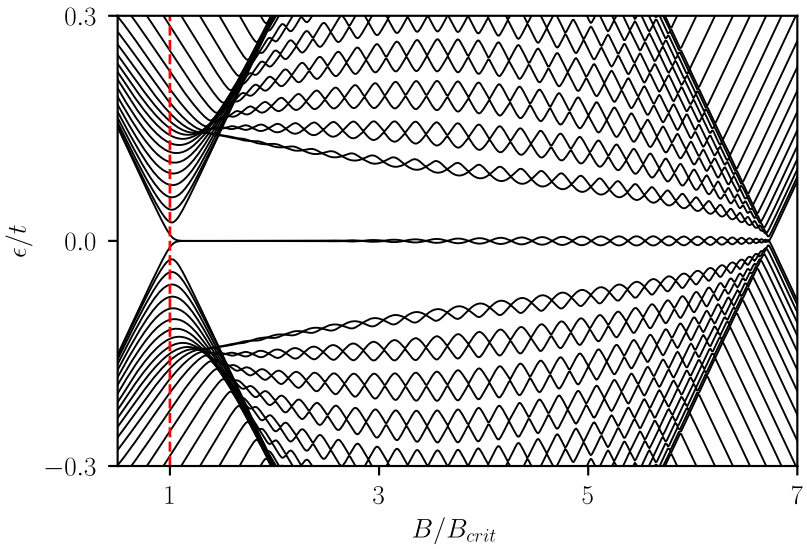

Figure 2.3: BdG excitation spectrum of a homogeneous-SOC chain ($N = 50$ sites) for increasing magnetic field in the z direction. Simulation parameters (in units of t): $t_{SO_x} = t_{SO_y} = 0.2,\ \mu = 0,\ \Delta = 0.3$. The dashed vertical line indicates the point corresponding to the topological phase transition.

The spectrum certainly resembles that of the Kitaev chain (Fig. 1.1a). In like manner, it is symmetric around zero energy due to the particle-hole symmetry induced by the BdG formalism, and more importantly, a zero-energy excitation emerges in the middle of a gap once the topological phase is reached, i.e., for $B \geq B_c$.

Moreover, a second topological phase transition occurs at $B \sim 6.5B_c$, which we did not encounter during the analytical analysis. This result is inherent in the tight-binding model, and can be explained invoking the bulk-edge correspondence argument: if we Fourier-transformed the Hamiltonian in Eq. (2.12), we would recover a finite band structure, similar to the one obtained for the Kitaev model (recall Eq. (1.13)). Likewise, the periodic band structure would undergo a second topological phase transition corresponding to the gap-closing at $k = \pi$, which is what we observe in the plot. This apparent mismatch should not cause any uneasiness to the reader, since that magnetic energy [1] is far beyond the attainable values in a laboratory; however, it shows the limitations of our model and one should always bear in mind, that in reality, the spectrum is not of infinite band-width as we obtained earlier.

The last remarkable feature of the plot in Figure 2.3 are the oscillations of the zero-energy excitation above certain magnetic field. This phenomenon is a finite size effect which corresponds to the overlapping of the Majorana wavefunctions [9, 11].

[1] For a typical laboratory magnetic field (~ 30 T) we have $B = g\mu_B\mathcal{B}/2 \sim 4 \cdot 10^{-5}$ meV $\ll 6.5B_c \sim 1.6$ meV [11].

Chapter 3

The Rashba nanowire: inhomogeneous spin-orbit coupling

The previous survey on the wonted Rashba nanowire has prepared the ground for the bulk of this work, so we will now delve into the study of an inhomogeneous spin-orbit interaction. Our main goal will be to investigate whether a defect in the spin-orbit coupling is sufficient to localize the Majorana zero modes, provided the wire is in the topological phase.

As a consequence of the newly incorporated inhomogeneity, the translational invariance of the system is irremediably lost and studying the spectrum in momentum space is not a feasible option anymore. In addition, analytical calculations are now extremely challenging, if not beyond the bounds of possibility; therefore, we are left with numerical analysis as the only tool to tackle the problem.

To our knowledge, the 1D case has not been studied in depth and only Klinovaja and Loss [12] had written on the subject previously. Nevertheless, this End-of-Degree Thesis does not aspire to provide a comprehensive picture of the matter, and we will content ourselves with exploring a few details.

3.1 Modelling the inhomogeneity

In Chapter 3 we chose the Rashba field to lie on the x-y plane (*cf.* Eqs. (2.3) and (2.12)). Henceforth, we will allow the angle θ with the x-axis to vary along the wire, letting the spin-orbit coupling vector rotate on its plane.

The tight-binding Hamiltonian of the system is practically that of the homogeneous case displayed in Eq. (2.12), except for the spin-orbit coupling parameters being reformulated as follows:

$$t_{SO_x}(j) = t_{SO}\cos\theta(j), \qquad t_{SO_y}(j) = t_{SO}\sin\theta(j), \tag{3.1}$$

where the phase describes a hyperbolic tangent profile:

$$\theta(j) = w\pi \left[\tanh\left(\frac{j + 1/2 - j_0}{\lambda} \right) + \tanh\left(-\frac{j + 1/2 - j_1}{\lambda} \right) \right]. \tag{3.2}$$

In doing so, four new parameters are introduced in the Hamiltonian: λ, which represents the *characteristic length* along which the rotation is performed, the *winding parameter* w, which indicates the number of turns the SOC-vector does at each defect, and j_0 and j_1, which will allow us to localise the rotations.

We have chosen to insert two rotations to avoid any discontinuities in the periodic boundary conditions scheme. We shall refer to the defect located at j_0 as *kink* and use *anti-kink* for its counterpart at j_1. Moreover, note that the SOC hopping parameters are effectively evaluated at $j + 1/2$. It was decided to implement the inhomogeneity in such manner to take into account the fact that the spin-orbit term involves two nearest neighbours in the tight-binding Hamiltonian (2.12).

Finally, it is worth mentioning that we shall distinguish between *abrupt* and *smooth* rotations. Within our numerical approach, we implement an abrupt rotation setting $\lambda << a$, being a the lattice spacing in the tight-binding model. However, this quantity is meaningless in an actual experimental arrangement, where several length-scales are involved. We shall assume that an abrupt rotation implies $\lambda << \lambda_F$, the Fermi wavelength [12].

3.2 Fermionic bound states

One of the main findings in [12] was that a zero energy mode, similar to the Majorana bound states, arises at the defect when the SOC vector undergoes a $w = 0.5$, *abrupt* rotation. Along this Section, we recover their result, in spite of having characterised the kinks slightly differently, and we examine how this feature is lost if the rotation is performed *smoothly*.

In order to exemplify these phenomena, we will focus on a closed chain so that the Majorana zero modes on the edges are discarded, hence simplifying the system. Implementing periodic boundary conditions in our Hamiltonian only requires to extend the second summation in Eq. (2.12) to $N - 1$ and then set $C_N = C_0$, $C_N^\dagger = C_0^\dagger$.

The spectrum corresponding to the aforementioned case is plotted in Figure 3.1. At first glance, it appears that we recover a similar evolution to that of the homogeneous case (*cf.* Fig. 2.3), where the spectrum gaps at $B = B_{crit}$, giving birth to some intra-gap, zero-energy states. However, one should recall that in this case we performed the calculations in a closed chain where there are not any edges, and therefore any topological phase-vacuum interfaces either. Indeed, these *fermionic bound states* resemble the Majorana zero modes, but actually, they are localized at the SOC defects (Fig. 3.2). They come in a pair due to the fact that we implemented two defects (kink and anti-kink) in our chain and it was found that their difference in energy decreases exponentially with the size of the system, suggesting that in the thermodynamic limit one would find a doubly degenerated excitation.

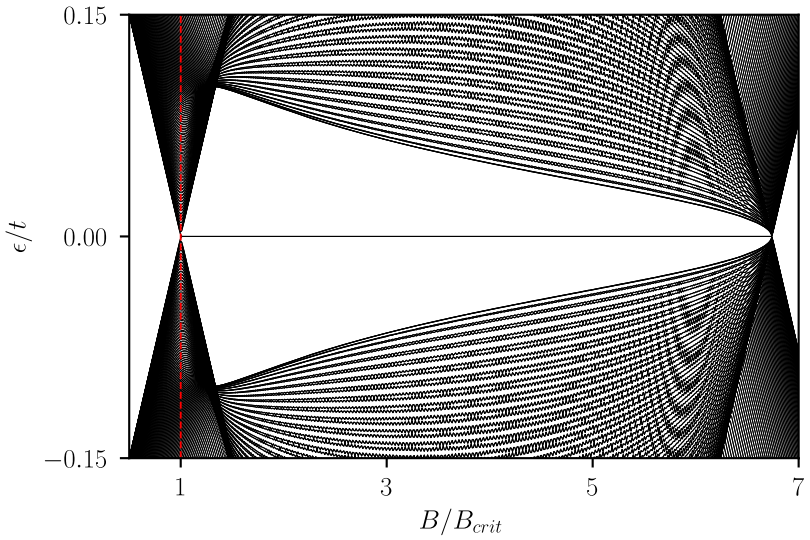

Figure 3.1: BdG excitation spectrum of an inhomogeneous-SOC chain ($N = 500$ sites, PBC) for increasing magnetic field in the z direction. Simulation parameters: $t_{SO} = 1,\ \mu = 0,\ \Delta = 0.3$ (in units of t); $\lambda = 0.1a,\ j_0 = 125,\ j_1 = 375,\ w = 0.5$. The dashed vertical line indicates the topological phase transition. Since the chain is substantially longer than that of the spectrum in Fig. 2.3, there are not any oscillations or other noticeable finite-size effects.

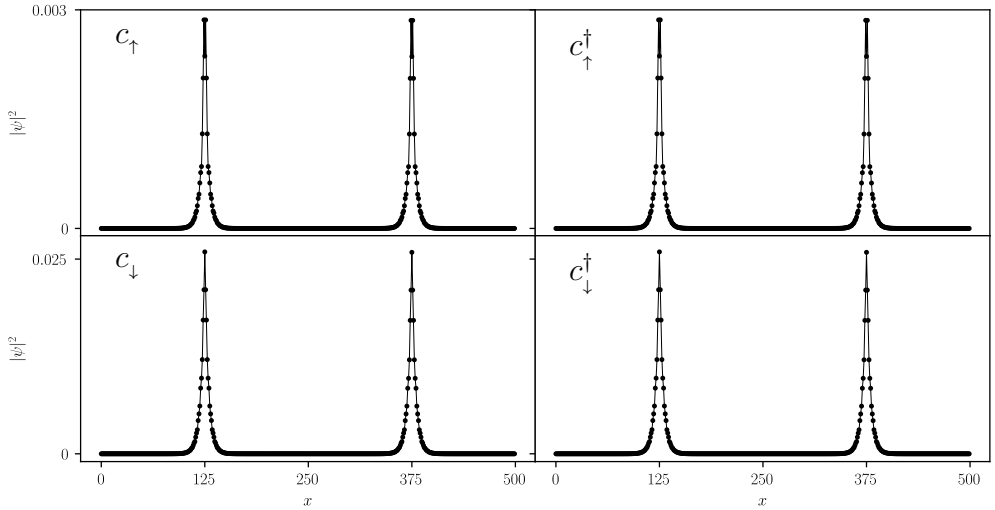

Figure 3.2: Eigenmode corresponding to one of the two zero-energy excitations for the inhomogeneous-SOC chain at $B = 2B_c$. The rest of the parameters are those of the above plot. The other zero-energy excitation was omitted as it exhibits the same behaviour. Chosen basis: $C^\dagger = (c_\uparrow^\dagger, c_\downarrow^\dagger, c_\downarrow, -c_\uparrow)$. There exists a difference of one order of magnitude in the probability maxima between spin-up and spin-down components, but given the Zeeman term in the Hamiltonian one should not expect the two species to behave equivalently.

These new intra-gap excitations are not as robust as the original Majorana zero modes, and a slight displacement from $w = 0.5$ lifts the excitation from its privileged position at zero energy, albeit recovered for any $w = n + 0.5$ with $n \in \mathbb{Z}$ (Fig. 3.3a).

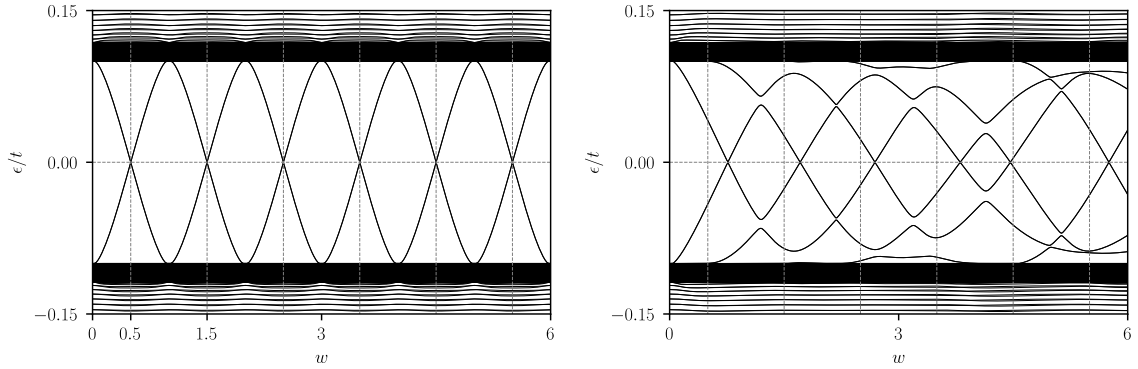

(a) Case of an *abrupt* rotation ($\lambda = 0.1a$). (b) Case of a *smooth* rotation ($\lambda = 2a$).

Figure 3.3: BdG excitation spectrum of an inhomogeneous-SOC chain ($N = 500$ sites, PBC) in the topological phase as a function of the winding parameter w, where $w = 1$ represents a full rotation of the SOC vector. Simulation parameters: $t_{SO} = 0.2,\ \mu = 0,\ B = 0.4,\ \Delta = 0.3$ (in units of t); $j_0 = 125,\ j_1 = 375$.

Quite remarkably, this periodicity is lost as soon as we implement a smooth defect (Fig. 3.3b). In order to explain this surprising behaviour, we propose the following heuristic argument: in the case of an *abrupt* rotation, i.e. $\lambda \to 0$, it is reasonable to admit that in Eq. (3.2), $\tanh\left(\pm\frac{j+1/2-j_{0,1}}{\lambda}\right) \approx \pm 1\ \forall j$, which implies that the Hamiltonian is equivalent for any $w,\ w'$, provided that $\max\{w, w'\}/\min\{w, w'\} = n \in \mathbb{Z}$. However, in the case of a *smooth* rotation the previous assumption is no longer valid, and as a consequence the parameters $t_{SO_{x,y}}(j)$ have different periodicity in w depending on the value of j. In other words, the Hamiltonian does not follow the previous equivalence rule and there is not any reason to expect a periodic behaviour in w. Interestingly, the number of zero-energy crossings appears to be equal in both regimes, but they do not represent exactly the same: in the *abrupt* case, a zero-energy crossing indicates that, for such w, there is a mid-gap excitation for any B within the topological phase, while in the *smooth* case, the w corresponding to the crossing also depends on the magnetic field. Alas, numerical analysis does not allow to gain further insight into this direction.

Trivial-topological interface

At this point, one might argue that in the preceding analysis we did not find "proper" Majorana zero modes because we did not have any interface between a trivial and a topological phase, unlike in the Kitaev chain, where the vacuum behaves as a trivial phase. This can be easily achieved rotating the magnetic field so that it lays along the y axis. Now, we can implement a rotation which leaves the SOC field parallel to the magnetic field, and thereby engineering a nanowire which is half-topological and half-trivial. However, this scheme does not yield any satisfactory results. As it can be seen in Fig. 3.4, any potential MZM on the domain wall would mix with the bulk state in the trivial phase.

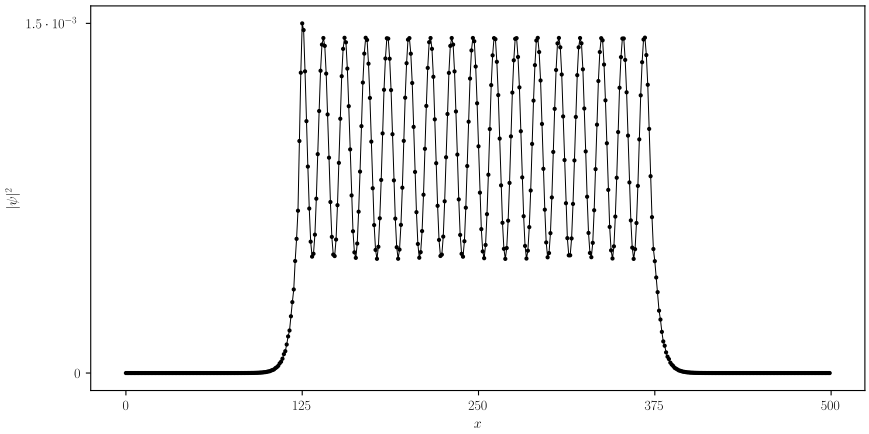

Figure 3.4: First BdG excitation ($c^\dagger_\downarrow$) for the inhomogeneous-SOC chain ($N = 500$, PBC). Simulation parameters: $t_{SO} = 0.2,\ \mu = 0, B = 2B_c,\ \Delta = 0.3$ (in units of t); $j_0 = 125,\ j_1 = 375,\ w = 0.75,\ \lambda = 0.01a$. The magnetic field is aligned along y, and it is parallel to the SOC vector from the sites 125 to 375.

3.3 Majorana zero modes and fermionic bound states

Throughout the preceding Section, in order to better understand the role played by the inhomogeneity in the spin-orbit coupling, we steered clear of any kind of edge physics considering a closed chain. The next natural step would be to wonder whether the introduced defect has any repercussions on the original Majorana zero modes which we had engineered in the homogeneous Rashba nanowire.

In general, when we examined an open chain with the kink/anti-kink structure in the spin-orbit coupling, we found that the defect hardly affected the Majorana zero modes. Nevertheless, in the case of a $w = 1$, *smooth* rotation an interesting finite-size effect takes place which is worth reporting.

For low magnetic fields (Fig. 3.5, bottom row), the first BdG excitation corresponds to the Majorana zero modes localized on the edges, in the same manner that we found in the Kitaev chain, or equivalently, in the homogeneous Rashba nanowire. The first and second BdG excitations are anchored at the defects, although for the present choice of parameters ($w = 1,\ \lambda = 10a$) they have a finite energy. For high values of B (Fig. 3.5, top row) the MZMs delocalize into the bulk of the chain. This effect was also observed during the study of the homogeneous case, where for a sufficiently high magnetic field, the MZMs exhibited an oscillatory behaviour (*cf.* Fig. 2.3). However, an unexpected phenomenon occurs at intermediate magnetic field: when $B \sim 2.7B_{crit}$ the first BdG excitation appears to be pinned at the defects, whereas the first a second BdG excitations delocalize toward the edges. Strikingly, the Majorana zero modes are somewhat recovered for a higher magnetic field (Fig. 3.5, third row).

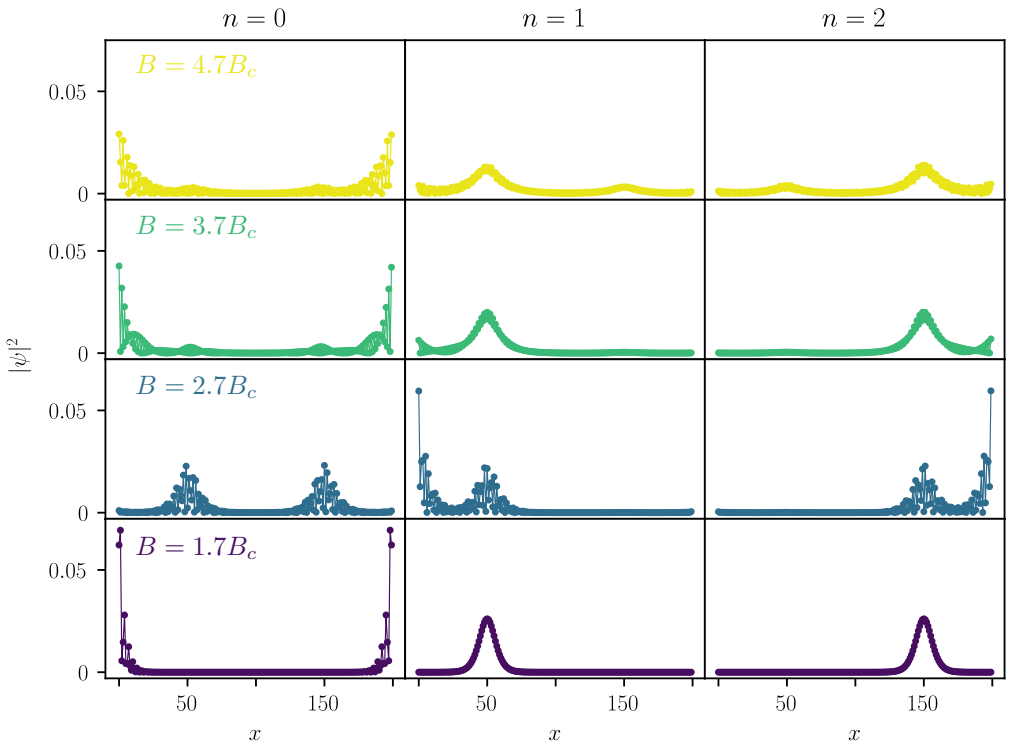

Figure 3.5: BdG excitation eigenmodes of an inhomogeneous-SOC chain ($N = 200$ sites, OBC), for different values of magnetic field in the z direction. Simulation parameters: $t_{SO} = 0.2$, $\mu = 0$, $\Delta = 0.3$ (in units of t); $\lambda = 10a$, $j_0 = 50$, $j_1 = 150$, $w = 1$. The left, middle and right columns correspond to the three first BdG excitations in energy, respectively. For brevity, only the spin-down electron ($c^\dagger_\downarrow$) excitations are depicted, the other components exhibiting a similar behaviour.

In order to try to explain this behaviour, we shall consider separately an open, homogeneous system which only hosts Majorana zero modes on the edges, and a closed inhomogeneous chain which only allows the existence of fermionic bound states. Inspired by first-order perturbation theory, we computed the overlap between the first BdG excitations of the two systems, and their difference in energy (Fig. 3.6).

Interestingly, we found that in the case of a relatively small chain ($N = 200$) the overlap is non-zero. However, in perturbation theory such overlap is only relevant when the difference in energy is small compared to the energy scale of the problem. In our present state of affairs, it is not evident which is such energy scale, but in any case, the numerical analysis allows us to observe that $E_{k/a} - E_{hom} \simeq E_{k/a}$ vanishes for the same magnetic field which led to the "mixing" of the eigenfunctions, providing a plausible explanation. On the other hand, the overlap is non-existent when we consider a longer chain ($N = 800$), for which the effect discussed above was not observed.

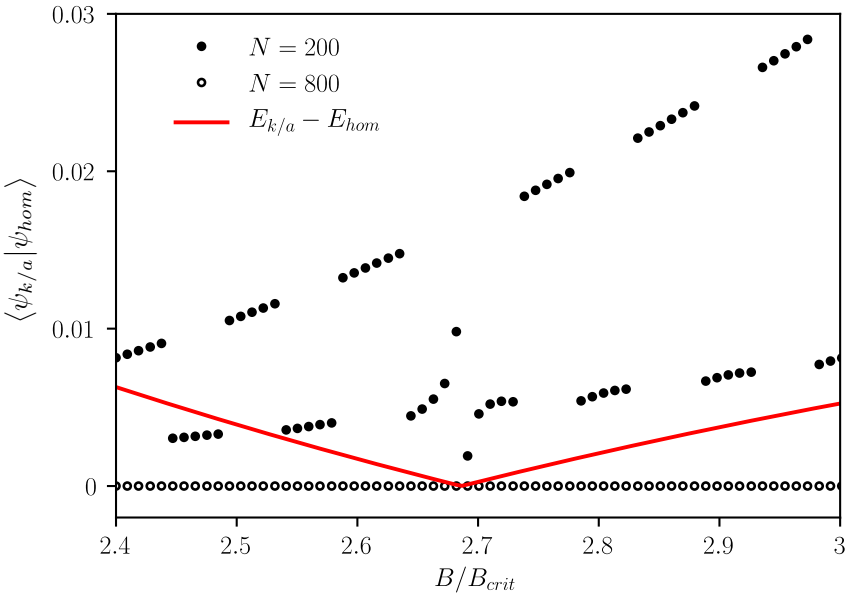

Figure 3.6: Overlap of the first BdG excitations of an open homogeneous system and a kink/anti-kink scheme with PBC as a function of the magnetic field. The solid line represents the energy difference of the excitations (which does not depend on N) in units of t. Simulation parameters: $t_{SO} = 0.2,\ \mu = 0,\ \Delta = 0.3$ (in units of t); $\lambda = 10a,\ j_0 = N/4,\ j_1 = 3N/4,\ w = 1$

Chapter 4

Conclusions and outlook

Along this End-of Degree Thesis, we examined thoroughly the homogeneous Rashba nanowire, a realistic arrangement which emulates a one-dimensional p-wave superconductor by integrating three widely accessible elements: spin-orbit coupling, a Zeeman field and s-wave superconductivity. Combining analytical and numerical methods, we reviewed how the system enters a topological phase characterised by the presence of isolated Majorana zero modes. This transition occurs at a precise critical magnetic field, which only depends on the chemical potential and the superconducting gap.

In the second instance, we studied the effect of an inhomogeneous spin-orbit coupling in the Rashba nanowire. We concluded that the defect is not enough to localize the Majorana zero modes, although there exists a specific type of domain wall (abrupt and winding parameter $w = 0.5$) which allows the existence of zero-energy fermionic bound states, akin to the Majorana zero modes. Numerical analysis allowed us to observe that, in general, the defect does not affect the MZMs on the edges, except in relatively small chains, where under certain conditions, the overlap of the MZM's and the fermionic bound states is not negligible.

The numerical approach with which we chose to tackle the inhomogeneous scheme definitely provided some flavour of the physics involved in the system, however, a profound and complete comprehension of the matter would require overcoming the problem analytically. Unfortunately, understanding why the FBSs only arise at $w = 0.5$, or the connexion between the spectra for abrupt and smooth defects is not achievable by merely considering the methods presented in this work.

Furthermore, several other aspects remain unexplored. It may be worthwhile to survey the possible differences between strong and weak spin-orbit regimes. More ambitiously, one could perform a comparative study of the inhomogeneous nanowire and its two-dimensional analogue, a vortex-like topological defect in spin-orbit coupling, where the existence of a MZM pair has been reported [13]. Finally, it could be of interest to try to elucidate whether the presence of fermionic bound states influences in some manner the exchange statistics of the Majorana zero modes.

Bibliography

[1] C. Beenakker, "Search for majorana fermions in superconductors," *Annu. Rev. Condens. Matter Phys.*, vol. 4, no. 1, pp. 113–136, 2013.

[2] M. Leijnse and K. Flensberg, "Introduction to topological superconductivity and majorana fermions," *Semiconductor Science and Technology*, vol. 27, no. 12, p. 124003, 2012.

[3] J. Alicea, "New directions in the pursuit of majorana fermions in solid state systems," *Reports on Progress in Physics*, vol. 75, no. 7, p. 076501, 2012.

[4] A. Y. Kitaev, "Unpaired majorana fermions in quantum wires," *Physics-Uspekhi*, vol. 44, no. 10S, p. 131, 2001.

[5] L. Fu and C. L. Kane, "Superconducting proximity effect and majorana fermions at the surface of a topological insulator," *Physical review letters*, vol. 100, no. 9, p. 096407, 2008.

[6] J. D. Sau, R. M. Lutchyn, S. Tewari, and S. Das Sarma, "Generic new platform for topological quantum computation using semiconductor heterostructures," *Phys. Rev. Lett.*, vol. 104, p. 040502, Jan 2010.

[7] R. M. Lutchyn, J. D. Sau, and S. D. Sarma, "Majorana fermions and a topological phase transition in semiconductor-superconductor heterostructures," *Physical review letters*, vol. 105, no. 7, p. 077001, 2010.

[8] Y. Oreg, G. Refael, and F. von Oppen, "Helical liquids and majorana bound states in quantum wires," *Phys. Rev. Lett.*, vol. 105, p. 177002, Oct 2010.

[9] R. Aguado, "Majorana quasiparticles in condensed matter," *Rivista del Nuovo Cimento*, vol. 40, 2017.

[10] A. Akhmerov, J. Sau, B. van Heck, S. Rubbert, and R. Skolasiński, *TU Delft TOPOCMx*. TU Delft Online Learning, 2014.

[11] J. Cayao, *Hybrid superconductor-semiconductor nanowire junctions as useful platforms to study Majorana bound states*. Universidad Autónoma de Madrid, 2016.

[12] J. Klinovaja and D. Loss, "Fermionic and majorana bound states in hybrid nanowires with non-uniform spin-orbit interaction," *The European Physical Journal B*, vol. 88, no. 3, p. 62, 2015.

[13] G. C. Ménard, A. Mesaros, C. Brun, F. Debontridder, D. Roditchev, P. Simon, and T. Cren, "Isolated pairs of majorana zero modes in a disordered superconducting lead monolayer," *Nature Communications*, vol. 10, no. 1, p. 2587, 2019.